LIMNOLOGY
and
OCEANOGRAPHY: METHODS

Limnol. Oceanogr.: Methods 9, 2011, 29–41

Estimating turbulent diffusion in a benthic boundary layer

Moritz Holtappels[1]* *and Andreas Lorke*[2]
[1]Max Planck Institute for Marine Microbiology, Celsiusstrasse 1, 28359 Bremen
[2]Institute of Environmental Sciences, University of Koblenz-Landau, Fortstrasse 7, 76829 Landau

Abstract

In aquatic environments, the benthic boundary layer (BBL) is the transition zone for dissolved solutes that are released or consumed from the sediments. The exchange of solutes between the sediment and the overlying water column depends on the turbulent transport in the benthic boundary layer. In situ measurements of turbulent diffusion in natural benthic boundary layers are scarce and are usually derived from the logarithmic law of the wall (log-law). Based on G. I. Taylor's turbulent diffusion theory, we derived a simple approach to estimate turbulent diffusivity from acoustic Doppler velocimeter (ADV) data. The approach was applied to ADV data collected over a period of 155 h in the BBL of Lake Constance, Germany. The calculated turbulent diffusivities agreed well with those derived in parallel from flux-gradient measurements. In addition, turbulent diffusivities were calculated from several established approaches, including those based on the logarithmic law of the wall. The log-law failed to predict plausible diffusivities whenever the boundary flow exhibited decreased current velocities or stable density stratification. Under these conditions, the turbulent diffusivities calculated from the flux-gradient measurement and from Taylor's theory were as low as 10^{-6} m^2 s^{-1}. These decreased turbulent diffusivities have the potential to control the solute exchange between the sediment and the water column and can result in low oxygen concentrations in the bottom water. Reliable measurements of turbulent diffusivities in the BBL are therefore important to investigate and predict hypoxia in bottom waters and sulfide efflux from the sediments.

In the shallow waters of lakes and the coastal ocean, primary productivity is strongly linked to the mineralization of organic matter in the sediments and thus to the exchange of organic matter, nutrients, and metabolites between sediments and water column (Wollast 1991). The benthic boundary layer (BBL) is the interface between the sediments and the water column. By definition, it is the water layer that is influenced by the friction between the sediment and the moving water column (Dade et al. 2001). The vertical transport of solutes and particulate matter across the BBL is of turbulent nature. Assuming stationary conditions and neglecting the reactivity of the solute in the BBL, the turbulent transport of solutes can be described as quasi diffusive transport according to Fick's law of diffusion:

$$J = -D_T \frac{\partial C}{\partial z} \quad (1)$$

where J denotes the flux, D_T is the turbulent diffusivity, and $\partial C/\partial z$ is the vertical concentration gradient. Turbulent transport in the BBL is believed to be several orders of magnitude faster compared with molecular diffusion in the sediments. In contrast to molecular diffusion, turbulent diffusion is a function of the flow field and, therefore, varies with the flow velocity in the BBL. There are numerous models in which turbulent diffusivity scales as a function of boundary distance and mean current velocity (Dade et al. 2001). The most common model is the logarithmic law of the wall (i.e., log-law) (von Kármán 1930), verified in various laboratory flume experiments (Pope 2000).

However, measurements of turbulent diffusivity in natural boundary flows are scarce. Theoretical constraints from the log-law, such as the linear increase of D_T with shear velocity u_* and distance to the boundary z ($D_T = u_* \kappa z$) suggest that the turbulent transport in the BBL is too fast to limit the oxygen and nutrient fluxes across the sediment-water interface (Boudreau 2001) and, in this respect, turbulent diffusivity may be seen as a parameter of minor interest. We give two reasons why the measurement of turbulent diffusivity in the BBL is of interest. First, Sauter et al. (2005) and Holtappels et al. (2010) recently demonstrated that nutrient and oxygen gradients in the BBL are measureable. With the knowledge of the turbulent diffu-

*Corresponding author: E-mail: mholtapp@mpi-bremen.de

Acknowledgment

We thank Lars Umlauf and Volker Mohrholz for ideas and preparation of the measurement campaign as well as Christian Noss for advice and fruitful discussions. We gratefully acknowledge the help of the crew of the RV *Robert Lauterborn* during field work at Lake Constance. This study was funded through DFG-Research Center/Excellence Cluster, "The Ocean in the Earth System," the Max Planck Society, and the German Research Foundation (grant Lo1150/3-1).

DOI 10.4319/lom.2011.9.29

sivity, it becomes possible to calculate the respective solute flux according to Fick's law (Eq. 1). This approach would provide a new noninvasive method to determine the solute fluxes across the sediment-water interface. Second, there is evidence that the log-law does not apply for conditions of low current velocities and stratified boundary layers (Brand et al. 2008; Lorke et al. 2002), which commonly occur in natural aquatic systems. Under these conditions, turbulent diffusivities as low as 10^{-7} m^2 s^{-1} (Lorke 2007) have been measured that potentially control the solute flux between the sediment and the water column. It is, therefore, imperative to (i) derive a convenient method to measure the turbulent diffusivity independent from the log law and (ii) measure the turbulent diffusivity at critical conditions such as low current velocities and stratification.

In this article, we present a new approach for measuring turbulent diffusivity. The approach is based on Taylor (1921) who described the quasi diffusive transport by continuous movements from statistical measures. We applied this theory to measure turbulent diffusivities in the benthic boundary layer of Lake Constance, Germany. We compared the turbulent diffusivities with those derived from density gradient and density flux measurements according to Fick's law. Furthermore, we tested three approaches based on the log-law as well as turbulent diffusivities derived from the concept of turbulent viscosity and from Osborn's (1980) equation for turbulence in stratified flows. We discuss the results in the context of the measured current velocity and density stratification in the BBL.

Materials and procedures

In this section, we present the theoretical concepts of different approaches that were applied to calculate turbulent diffusivity in the benthic boundary layer of Lake Constance.

Turbulent diffusivity derived from Taylor's theory

In stationary, homogenous turbulence, the mean square displacement $\langle X^2 \rangle$ of a fluid parcel at elapsed time t due to its fluctuation velocities u_L is expressed according to Taylor (1921) as

$$\left\langle X^2 \right\rangle = 2 \cdot \left\langle u_L^2 \right\rangle \cdot t \cdot \int_0^\infty R_L(\tau)\, d\tau \tag{2}$$

Here, and in the following, the instantaneous velocity U_L is decomposed into a mean velocity $\bar{U}_L$ and a fluctuating velocity u_L according to $U_L = \bar{U}_L + u_L$. Lagrangian and Eulerian velocities are denoted as U_L and U, respectively. The normalized Lagrangian autocorrelation coefficient R_L is defined as

$$R_L = \frac{\langle u_L(t) \cdot u_L(t+\tau) \rangle}{\left\langle u_L^2 \right\rangle} \tag{3}$$

with the time interval τ. For $\tau = 0$, R_L equals 1 and for $\tau \to \infty$, R_L approaches 0. The integral of R_L is called the Lagrangian integral time scale

$$T_L = \int_0^\infty R_L(\tau)\, d\tau ,$$

which approaches a constant value for $\tau \to \infty$ (Taylor 1921). T_L represents the characteristic time interval over which the instantaneous velocity of the fluid parcel is correlated with its previous velocities. For $t >> T_L$, the mean square displacement $\langle X^2 \rangle$ in Eq. 2 is a linear function of t, thus characterizing a diffusive process. The turbulent diffusion coefficient is defined as $D_T = \left\langle X^2 \right\rangle / 2t$ and from Eq. 2, we obtain:

$$D_T = \left\langle u_L^2 \right\rangle \cdot T_L \tag{4}$$

The Lagrangian integral length scale L_L is defined by (Tennekes and Lumley 1972)

$$L_L = u_L' \cdot T_L \tag{5}$$

with u_L' as the standard deviation of u_L. We can write Eq. 4 as

$$D_T = u_L' \cdot L_L \tag{6}$$

Equation 2 was verified experimentally by Sato and Yamamoto (1987) using Lagrangian particle tracking. However, in the BBL, velocities are usually measured in the Eulerian reference frame at a fixed position above the sediment. Turbulent flow is measured as it floats past the velocity sensor with the mean flow. A velocity sensor would have to move with the mean flow to derive a time series of turbulent velocities within an eddy. A fixed senor, therefore, measures a mixture of a spatial transect through the flow and a time series. According to Taylor's hypothesis (1938), the rate of change of a turbulent eddy is small compared with the velocity of the mean flow $\bar{U}$, so that the turbulence can be considered as 'frozen,' as it passes by the sensor. Therefore, the time interval τ between two consecutive velocity measurements of the sensor can be translated into the spatial distance $r = \tau \cdot \bar{U}$ and the autocorrelation coefficient of the Eulerian velocity u translates into the Eulerian spatial correlation coefficient

$$E_E = \frac{\langle u(x) \cdot u(x+r) \rangle}{\left\langle u^2 \right\rangle} \tag{7}$$

The integral of E_E is called the Eulerian integral length scale (Tennekes and Lumley 1972)

$$L_E = \int_0^\infty E_E(r)\, dr \tag{8}$$

A common assumption is that $L_L \approx L_E$, and furthermore, it was shown that $u_L' = u'$ (Tennekes and Lumley 1972) so that the turbulent diffusion coefficient can be calculated from Eulerian velocities according to

$$D_T = u' \cdot L_E \tag{9}$$

In the benthic boundary layer, we assume a stationary boundary flow in which flow characteristics vary in the vertical scale but are homogeneous in the horizontal plane. In the following, we denote u, v, w as the x, y, z component of the fluctuating velocity

with the mean flow pointing toward x and the transversal and vertical flow toward y and z (positive z in upward direction), respectively. Because we are interested in the vertical diffusive transport across the turbulent boundary layer, the vertical turbulent diffusion coefficient was calculated according to Eq. 9:

$$D_T = w' L_E \tag{10}$$

In the following, the turbulent diffusion coefficient derived from Taylor's theory is denoted as D_{T_T}. D_{T_T} can be estimated from single point velocity measurements with a sampling frequency that is high enough to resolve turbulent motion.

Turbulent diffusivity derived from the concept of turbulent viscosity

In turbulent fluid flow, the shear stress due to turbulent fluctuations of fluid momentum is called Reynolds stress. A definition of the Reynolds stress (τ_{ij}) is derived from Reynolds averaging of the Navier-Stokes equations (Tennekes and Lumley 1972) which, in case of a boundary flow, results in:

$$\tau_{xz} = -\rho \langle u w \rangle \tag{11}$$

where ρ is the fluid density and $\langle uw \rangle$ is the time averaged covariance of the velocities in the mean flow direction (u) and vertical direction (w). In analogy to the shear stress in laminar flow, the Reynolds stress in turbulent shear flow is assumed to be proportional to the mean velocity gradient (Tennekes and Lumley 1972):

$$\langle u w \rangle = -\nu_T \frac{\partial \bar{U}}{\partial z} \tag{12}$$

where the constant of proportionality (ν_T) is denoted as turbulent viscosity or momentum diffusion coefficient. It is assumed that ν_T equals the turbulent diffusion coefficient for solutes (D_T) (Tennekes and Lumley 1972), so that

$$D_T = -\frac{\langle u w \rangle}{\partial \bar{U} / \partial z} \tag{13}$$

In the following, the turbulent diffusion coefficient derived from turbulent viscosity is denoted as D_{T_V}. To estimate D_{T_V}, it needs a high frequency single point velocity measurement together with a mean velocity profile. It should be mentioned that D_{T_T} and D_{T_V} are determined without any assumption regarding the structure of the boundary layer and are applicable also for free shear flows.

Turbulent diffusivity derived from the logarithmic law of the wall

Expressions of D_T that include the boundary dimensions are derived from the logarithmic law of the wall. In fully developed turbulent boundary flows the average velocity profile $\bar{U}(z)$ is described by the logarithmic law of the wall (von Kármán 1930):

$$\bar{U}(z) = \frac{u_*}{\kappa} \ln\left(\frac{z}{z_0}\right) \tag{14}$$

where κ is the von Kármán's constant (~0.41), z is the height above the bottom, and z_0 is the hydraulic roughness, a constant of integration found to increase with bottom roughness. The friction velocity u_* is related to the Reynolds stress (τ_{xz}) and the fluid density (ρ) according to $u_* = \sqrt{\tau_{xz} / \rho}$. Considering Eq. 11, it follows that

$$u_*^2 = -\langle u w \rangle \tag{15}$$

The logarithmic law of the wall applies to a specific range in the BBL defined by upper and lower boundaries. However, the boundaries themselves depend on the flow field. The lower boundary is set where direct effects of viscosity (ν) on the velocity gradient are negligible. Expressed in terms of viscosity and friction velocity, the lower boundary is set where $z > 30\,\nu / u_*$ (Pope 2000). The log-law applies to about 30% of the total boundary layer thickness, which is defined as the value of z where $\bar{U}$ equals 99% of the free flow velocity (Pope 2000). In lakes and oceans with moderate current velocities of ~0.1 m s^{-1} the log-layer extends from a few centimeters to a few meters above the sediment (Wuest and Lorke 2003).

A fundamental assumption of the log-law is a constant Reynolds stress throughout the layer and a velocity gradient that is a reciprocal function of z:

$$\frac{\partial \bar{U}}{\partial z} = \frac{u_*}{\kappa z} \tag{16}$$

For the log-layer, we derive a specific solution for D_T by substituting Eqs. 15 and 16 into Eq. 13:

$$D_T(z) = u_* \kappa z \tag{17}$$

Hence in the log-layer, D_T increases linearly with distance to the sediment. A value for u_* is derived either from the Reynolds stress (Eq. 15) leading to

$$D_T(z) = \sqrt{-\langle u w \rangle}\, \kappa z \tag{18}$$

or from the mean velocity $\bar{U}$ (Eq. 14), which leads to

$$D_T(z) = \frac{\bar{U}(z) \kappa^2 z}{\ln(z / z_0)} \tag{19}$$

Yet another assumption that applies for the log-layer is the balance between the production rate of turbulent kinetic energy from shear stress (P) and the rate of energy dissipation (ε) by viscous shear (Kim et al. 2000; Tennekes and Lumley 1972):

$$-P + \varepsilon = -\langle u w \rangle \frac{\partial \bar{U}}{\partial z} + \varepsilon = 0 \tag{20}$$

Assuming the energy balance, we estimate D_T from ε by combining Eqs. 15, 16, 17, and 20:

$$D_T(z) = (\varepsilon \kappa z)^{1/3} \kappa z \tag{21}$$

In the following, the turbulent diffusion coefficients in the log-layer derived from Reynolds stress (Eq. 18), mean velocity (Eq. 19), and energy dissipation (Eq. 21) are denoted as D_{T_LR}, D_{T_LU}, and D_{T_LD}, respectively. A high frequency single point velocity measurement and the precise knowledge of z are sufficient to determine D_{T_LR} and D_{T_LD}, whereas D_{T_LU} is tied to the flow field only by the average flow velocity $\bar{U}$. However, for D_{T_LU} the hydraulic roughness z_0 needs to be estimated.

The assumed balance between production and dissipation of turbulent energy no longer holds true for boundary layers that exhibit density stratification. In this case, the energy balance needs to be reconsidered, because some energy is required for the buoyancy flux (Osborn 1980).

Turbulent diffusivity in stratified flows

In turbulent, stratified flows the turbulent diffusion coefficient of density can be estimated from the buoyancy flux and the density gradient according to (Osborn 1980):

$$D_T = \frac{J_b}{N^2} \tag{22}$$

with the buoyancy flux:

$$J_b = \frac{g}{\rho}\langle w\rho \rangle \tag{23}$$

and the Brunt-Väisälä frequency N, defined as:

$$N^2 = -\frac{g}{\rho}\frac{\partial \rho}{\partial z} \tag{24}$$

where g is the gravitational acceleration and $\langle w\rho \rangle$ is the covariance between the vertical velocity and the fluctuating density. Equaation 22 can be simplified to

$$D_T = -\frac{\langle w\rho \rangle}{\partial \rho / \partial z} \tag{25}$$

Here, $\langle w\rho \rangle$ expresses the instantaneous density flux averaged over a long time period. The flux is assumed proportional to the respective gradient, therewith defining the constant of proportionality as the turbulent diffusion coefficient (i.e., Fick's law of diffusion). In the following, D_T derived from combined flux and gradient measurements. In the following, D_T derived from combined flux and gradient measurements (Eq. 25) is denoted as D_{T_F}. Similar to D_{T_T} and D_{T_V}, D_{T_F} is not restricted to log-law conditions.

As mentioned before, energy is required for the buoyancy flux in stratified flows. Hence, the energy balance becomes $P = \varepsilon + J_b$. The flux Richardson number R_f is defined as the ratio of buoyancy flux to turbulent production ($R_f = J_b/P$) leading to

$$J_b = \left(\frac{R_f}{1 - R_f}\right)\varepsilon, \tag{26}$$

which is substituted into Eq. 22 to derive

$$D_T = \frac{\gamma \varepsilon}{N^2} \tag{27}$$

with the mixing coefficient $\gamma = R_f/(1 - R_f)$. Osborn (1980) found $\gamma \approx 0.2$, which was subsequently applied in various studies (Ivey et al. 2008; Wuest and Lorke 2003). In the following, D_T derived from Osborn's relation is denoted as D_{T_O}. D_{T_O} is only applicable in shear flows with stable stratification where buoyancy flux is at the expense of shear production. In contrast, D_{T_F} is also applicable in shear flow with density anomalies (i.e., unstable stratification), because both the density flux and the density gradient would change sign. Note that the negative sign in Eq. 24 and Eq. 25 is due to the upward pointing positive z-coordinate, which leads to a negative density gradient for a stable stratification. When the stratification is unstable the density gradient is positive and N^2 becomes negative. In this case, N cannot be interpreted as frequency anymore but can still be understood as a stratification parameter.

In this section, we introduced several approaches to determine D_T from various measurable quantities. Table 1 summarizes all approaches that were used for the following comparison. The in situ measurement, the specific data processing, and the results are described in the next section.

Assessment

Study site and sampling procedure

The measurements were conducted in Lake Constance, Germany (47°83′99 N, 9°81′89 E) in June 2007 (Fig. 1A). Lake Constance is a large (536 km²) monomictic lake that experiences a deep convective mixing during winter (December-March) and is thermally stratified during summer (June-October). The oscillatory current regime of Lake Constance is well described by Appt et al. (2004) and Lorke (2007). A mooring was deployed in the northwestern sub-basin (Lake Überlingen) at 100 m depth. The bottom slope at this depth is about 0.7°. As described in detail by Lorke et al. (2008), the mooring was equipped with a chain of 13 temperature loggers (TR-1050, RBR Ltd.), evenly distributed between 0.5 and 12.5 m above the bottom. Temperature was recorded every 10 s with a resolution of 5×10^{-5}°C. An acoustic Doppler velocimeter (ADV, Vector, Nortek AS) was mounted to the mooring with its sampling volume located 1 m above the bottom (Fig. 1B). A fast response thermistor (PME Inc.) was placed in the direct vicinity of the sampling volume. The ADV was operated in burst mode, sampling temperature, and current velocities for 256 s every 15 min with a sampling rate of 8 Hz. In addition, the mooring was equipped with an acoustic Doppler current profiler (ADCP, WH-600, RDI) operating in pulse coherent mode (RDI mode 5). The ADCP (Fig. 1B) resolved the near-bottom current velocity profile within 0.89 and 8.79 m above the sediment with a vertical resolution of 0.1 m and a sampling interval of 2.5 s. For further analysis, data from the ADCP and the temperature loggers were averaged over the burst interval of the ADV. The data set used in this study consisted of 620 bursts covering a time period of 155 h.

Data processing

For each burst, current velocities measured by the ADV and by the ADCP were rotated horizontally such that the mean

Table 1. A summary of approaches determining D_T in the BBL, grouped by their field of application.

Approach	Equation	(Nr)	Field of application
Taylor's	$D_{T\_T} = w' L_E$	(10)	Free shear flow
Fick's law	$D_T = -\frac{\langle w\rho \rangle}{\partial\rho / \partial z}$	(25)	Free shear flow
Turbulent viscosity	$D_{T\_V} = -\frac{\langle u w \rangle}{\partial \bar{U} / \partial z}$	(13)	Free shear flow
Osborn's	$D_{T\_O} = \frac{\gamma \varepsilon}{N^2}$	(27)	Stably, stratified free shear flow
Log-law Reynolds stress	$D_{T\_LR}(z) = \sqrt{-\langle u w \rangle}\,\kappa z$	(18)	Shear flow in log-layer
Log-law mean flow	$D_{T\_LU}(z) = \frac{\bar{U}(z)\kappa^2 z}{\ln(z / z_0)}$	(19)	Shear flow in log-layer
Log-law dissipation	$D_{T\_LD}(z) = (\varepsilon \kappa z)^{1/3} \kappa z$	(21)	Shear flow in log-layer

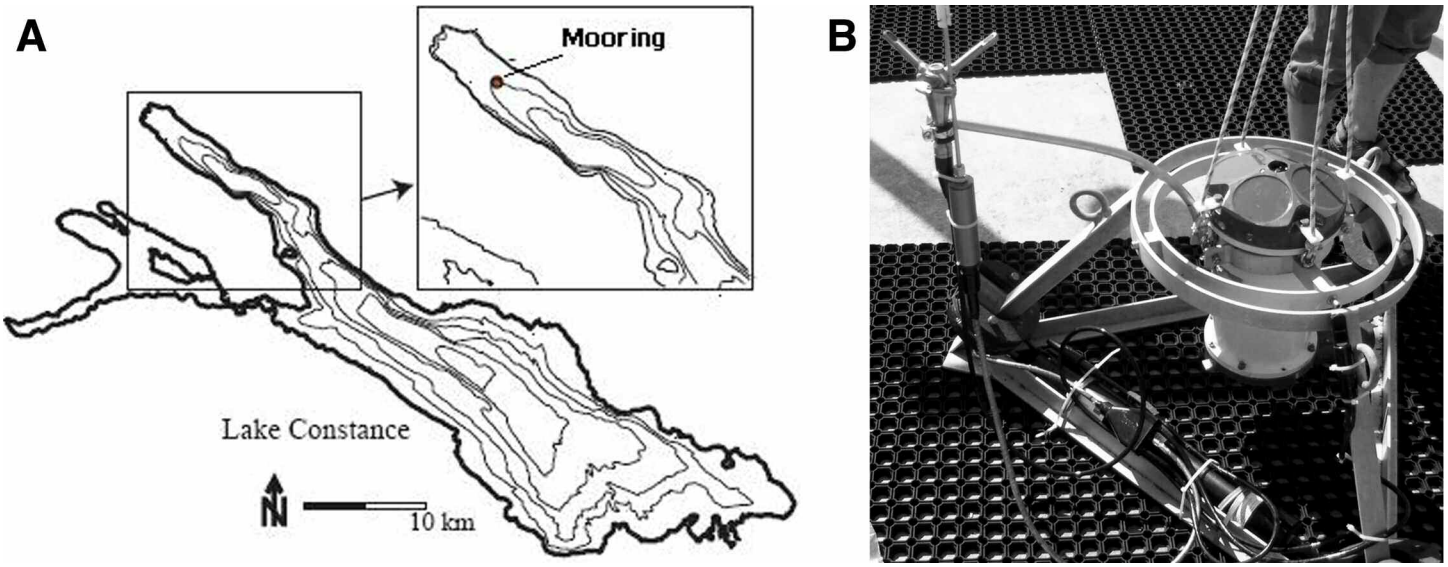

Fig. 1. (A) Map of Lake Constance. The mooring was deployed in the north-western sub basin (Lake Überlingen) at 100 m water depth. (B) A small tripod with upward-looking ADV and ADCP

flow vector was pointing along the x-axis. Subsequently, mean velocity $\bar{U}$ and standard deviations u', v', w' were calculated as well as the covariance $\langle uw \rangle$. From the fluctuating vertical velocity (w), we derived the Eulerian spatial correlation function and its integral, the Eulerian integral length scale (L_E), according to Eqs. 7 and 8. In detail, we used the Matlab function 'xcorr' to calculate the normalized autocorrelation coefficients for time intervals between 0 and 256 s (i.e., over the entire burst period). An example is shown in Fig. 2. The time intervals (τ) were translated into spatial distances $r = \tau \cdot \bar{U}$, which translates the autocorrelation coefficients into the Eulerian spatial correlation coefficients (E_E) (*see* Eq. 7). E_E was integrated over the spatial distance (r) using the Matlab function 'cumtrapz'. The integral length scale (L_E) was defined as the first maximum of the integrated E_E, which corresponds to the first zero crossing of the correlation coefficient. This criterion for the upper limit of integration was tested with time series of stochastic velocities of known integral timescales, which were calculated using the Langevin equation (Pope 2000). Integration of the autocorrelation functions until the first zero crossing compared well with the integral timescales used as input.

The energy dissipation rate (ε) was determined from frequency spectra of the vertical velocity w as described by Lorke and Wüest (2005). Briefly, the velocity frequency spectrum is

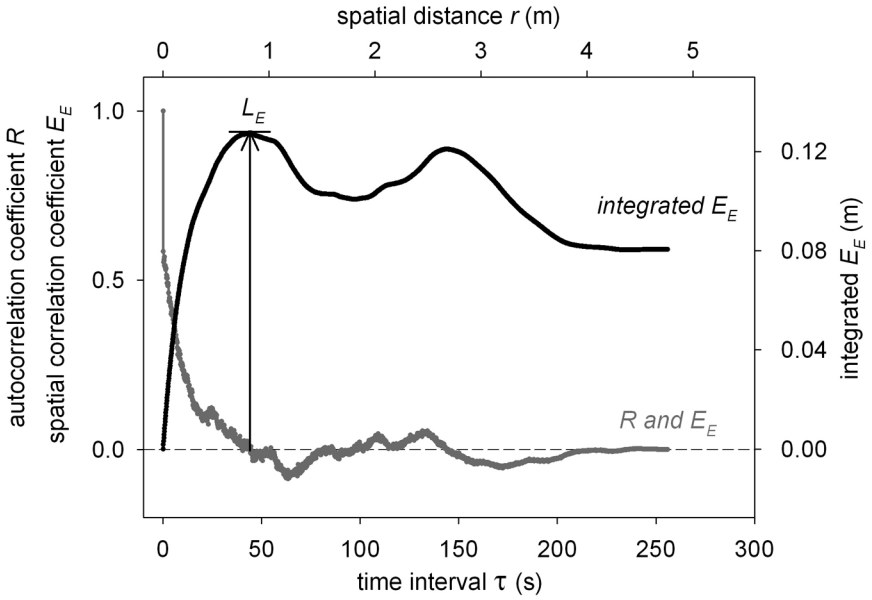

Fig. 2. Determination of L_E. The autocorrelation coefficient R is calculated as a function of the time interval τ (gray line). The time interval is translated into the spatial distance $r = \tau \cdot \bar{U}$ and the autocorrelation coefficient R translates into the spatial correlation coefficient E_E (for this burst, $\bar{U}$ = 0.0186 ms^{-1}). E_E is integrated over the spatial distance r (black line). The first maximum of the integrated E_E marks the first zero crossing of the correlation coefficient (arrow) and was chosen as the integral length scale L_E (here 0.127 m).

transferred into a wave number spectrum assuming Taylor's frozen turbulence hypothesis und subsequently fitted to the universal Kolmogorov spectrum: $\Phi = \alpha\, \varepsilon^{2/3}\, k^{-5/3}$ with the wavenumber k and the Kolmogorov constant for the vertical velocity $\alpha = 0.68$. The mean velocity gradient ($\partial\bar{U} / \partial z$) was calculated from velocities measured by the ADCP at 0.89 and 1.09 m above the sediment. In Lake Constance, variations in density are mainly caused by temperature variations. Therefore, the buoyancy flux was calculated from the covariance of temperature and vertical velocity, using the eddy correlation technique (Berg et al. 2003). Beforehand, temperatures were detrended by linear regression over the full burst period. The temperature gradient was calculated from the difference of mean temperature at 0.5 and 1.5 m above the sediment. The mixing coefficient γ (Eq. 27) was assumed to be 0.2 (Osborn 1980). The hydraulic roughness z_0 was estimated according to (Imboden and Wüest 1995):

$$z_0 = 0.1\, \nu / u_* \qquad (28)$$

with $u_* = (\varepsilon\, \kappa\, z)^{1/3}$ (*see* Eq. 21) averaged over all bursts and the kinematic viscosity (ν) of 1.52 × 10^{-6} m^2 s^{-1}. From the measured quantities all D_T's presented in Table 1 were calculated for each burst. To compare the different approaches we chose the Fickian approach (D_{T_F}) as reference (the reasons are discussed below). From a total of 620 bursts, we had to discard 140 bursts that showed temperature gradients below the accuracy of the thermistors (1 × 10^{-3}°C) and another 125 bursts with negative (i.e., not defined) D_{T_F}. In the following, we present the results of 353 bursts.

Results: Current regime and density structure in the BBL

Current velocities at 1 m above the sediment varied from a few millimeters per second up to 7 cm s^{-1} with an average of 2 cm s^{-1} (Fig. 3A). Current flow was predominantly in upslope (260-350°) and downslope (90-180°) direction (Fig. 3B, compare with Fig. 1A). The associated up- and downwelling caused significant changes of the mean temperature (Fig. 3C) and stratification (Fig. 3D). Temperatures decreased during upwelling and increased during downwelling over a range of 0.4°C. The temperature gradients at 1 m above the sediment varied from –10^{-2} to 10^{-1}°C m^{-1} (Fig. 3D). Negative temperature gradients imply that the water column was gravitational unstable (gray bars in Fig. 3), whereas positive temperature gradients denote stable stratification. Positive and negative temperature gradients were associated with downwelling and upwelling, respectively. Increased positive temperature gradients were found at low current velocities (see Lorke et al. 2008 for details).

Turbulent diffusivity in the BBL

The turbulent diffusion coefficients derived from heat fluxes and temperature gradients (Fick's first law, D_{T_F}) varied from 1 × 10^{-6} to 5 × 10^{-4} m^2 s^{-1} (Fig. 4A) after smoothing with a 1 h running average (i.e., 4 bursts). At time periods of unstable stratification and high current velocities (gray bars in Fig. 4) D_{T_F} maximized (>10^{-4} m^2 s^{-1}), whereas low current velocities and stable stratification led to reduced D_{T_F} (10^{-4} to 10^{-6} m^2 s^{-1}). Turbulent diffusivity derived from Taylor's hypothesis (D_{T_T} in Fig. 4A) agreed well with D_{T_F} and followed the trend of low diffusivities at stable stratification and high diffusivities and unstable stratification. The overall arithmetic mean of D_{T_F} (1.5 × 10^{-4} m^2 s^{-1}) and D_{T_T} (1.6 × 10^{-4} m^2 s^{-1}) were in good agreement.

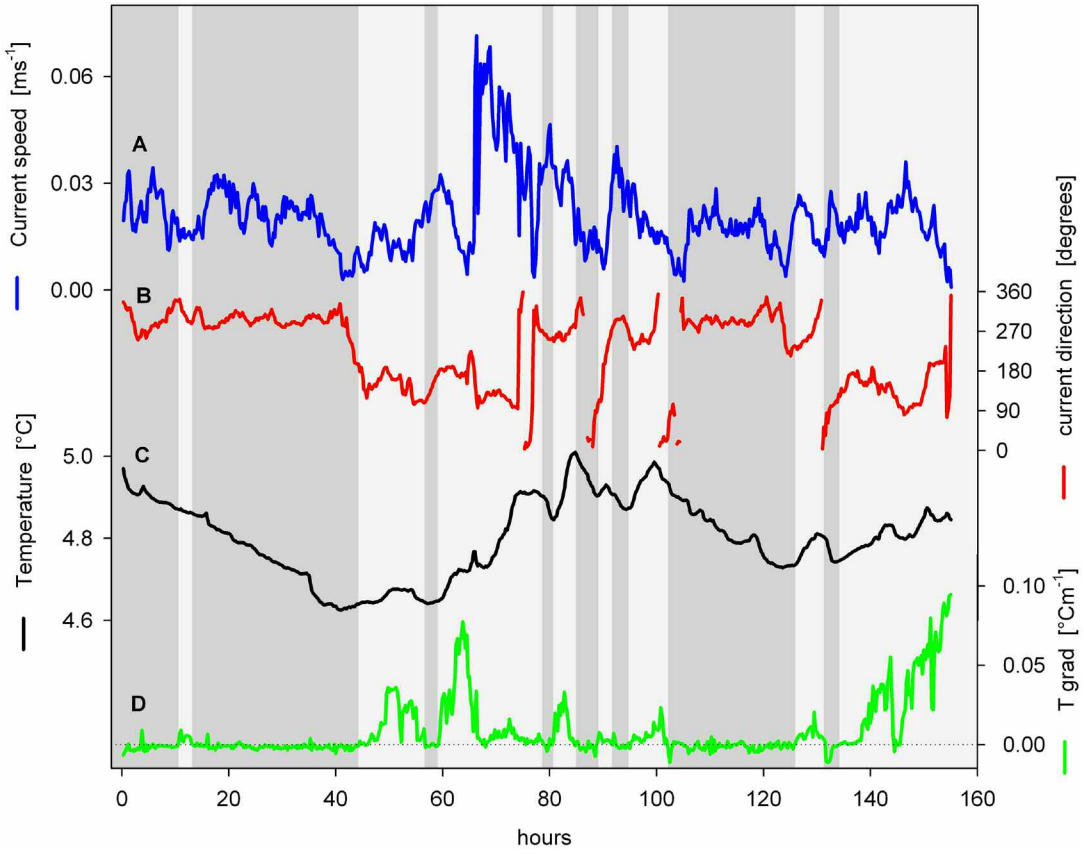

Fig. 3. (A + B) Current speed and direction measured 1 m above the sediment. Current directions were derived from north and east components of the current velocities measured by the ADCP. Upslope and downslope directions were north-west (260-350°) and south-east (90-180°), respectively. (C + D) Temperature at 0.5 m above the sediment and temperature gradient between 0.5 and 1.5 m above the sediment. The dotted line denotes zero temperature gradient. Time periods with gravitational unstable stratification (negative temperature gradients) are marked by gray bars.

A hydraulic roughness (z_0) of 4×10^{-4} m was derived from Eq. 28 and used to calculate D_{T_LU}. All diffusivities derived from the logarithmic law of the wall (D_{T_LD}, D_{T_LU}, and D_{T_LR} in Fig. 4B) were persistently at the upper boundary of D_{T_F} and did not reproduce the decrease of D_{T_F} during time periods of stable stratification and low current velocities (light gray bars in Fig. 4). Consequently, the temporal variability of D_{T_LD}, D_{T_LU}, and D_{T_LR} was decreased (10^{-3} to 10^{-4} m^2 s^{-1}) and the arithmetic mean was increased (3.9×10^{-4} to 4.8×10^{-4} m^2 s^{-1}) when compared with D_{T_F} and D_{T_T}. According to Eq. 18, D_{T_LR} was defined only for negative $\langle uw \rangle$. Bursts with positive $\langle uw \rangle$ were discarded, reducing the fraction of usable bursts to 65%. D_{T_LR} was similar to D_{T_LD} and D_{T_LU} except for increased D_{T_LR} at hour 42.

Diffusivity that was derived from turbulent viscosity (D_{T_V}) is defined for a negative ratio of $\langle uw \rangle$ to $\partial \bar{U} / \partial z$ only (see Eq. 13). D_{T_V} was defined for 64% of all bursts showing a high variability from 4×10^{-7} to 4×10^{-2} m^2 s^{-1} with considerable deviations from D_{T_F} (Fig. 4C). Maximized D_{T_V} was found at low current velocities, e.g., at hour 42, 125, and 153. Diffusivity that was derived from Osborn's equation (D_{T_O}) is defined for a positive temperature gradient only (Eq. 27 et seq.). D_{T_O} was calculated for 50% of all bursts and varied from 1×10^{-6} to 3×10^{-2} m^2 s^{-1} (Fig. 4C). D_{T_O} strongly deviated from D_{T_F} at decreased temperature gradients (hours 70-80, 100, and 130), whereas D_{T_O} agreed well with D_{T_F} when a stable stratification of the BBL was measured (hours 50, 63, and 140-150).

Factors determining turbulent diffusion:

The contribution of L_E and w' to D_{T_T} as well as the contribution of J_b and N^2 to D_{T_F} are shown in Fig. 5. The fluctuation of the vertical velocity, expressed by w' varied little between 1×10^{-3} and 4×10^{-3} m s^{-1}, whereas the integrated length scale L_E varied by a factor of 30 from 1 to 30 cm. Consequently, the variability of D_{T_T} was mainly determined by L_E. The Brunt-Väisälä frequency ($|N^2|$) and the buoyancy flux ($|J_b|$) in Fig. 5 were expressed in absolute values. $|N^2|$ varied over two orders of magnitude from 10^{-7} to 10^{-5} s^{-2}. The buoyancy flux varied from 5×10^{-12} to 10^{-9} W kg^{-1}. The variations of $|N^2|$ and $|J_b|$ were predominantly in phase causing little variations of D_{T_F}. The out of phase events at hour 10, 52, 90, and 142 resulted in rapid decrease of D_{T_F}. The energy dissipation rate (ε) ranged from 1×10^{-10} to 4×10^{-8} W kg^{-1} and was well correlated with the current velocity and the vertical velocity gradient but less correlated with Reynolds stress $\langle uw \rangle$. Time periods of increased

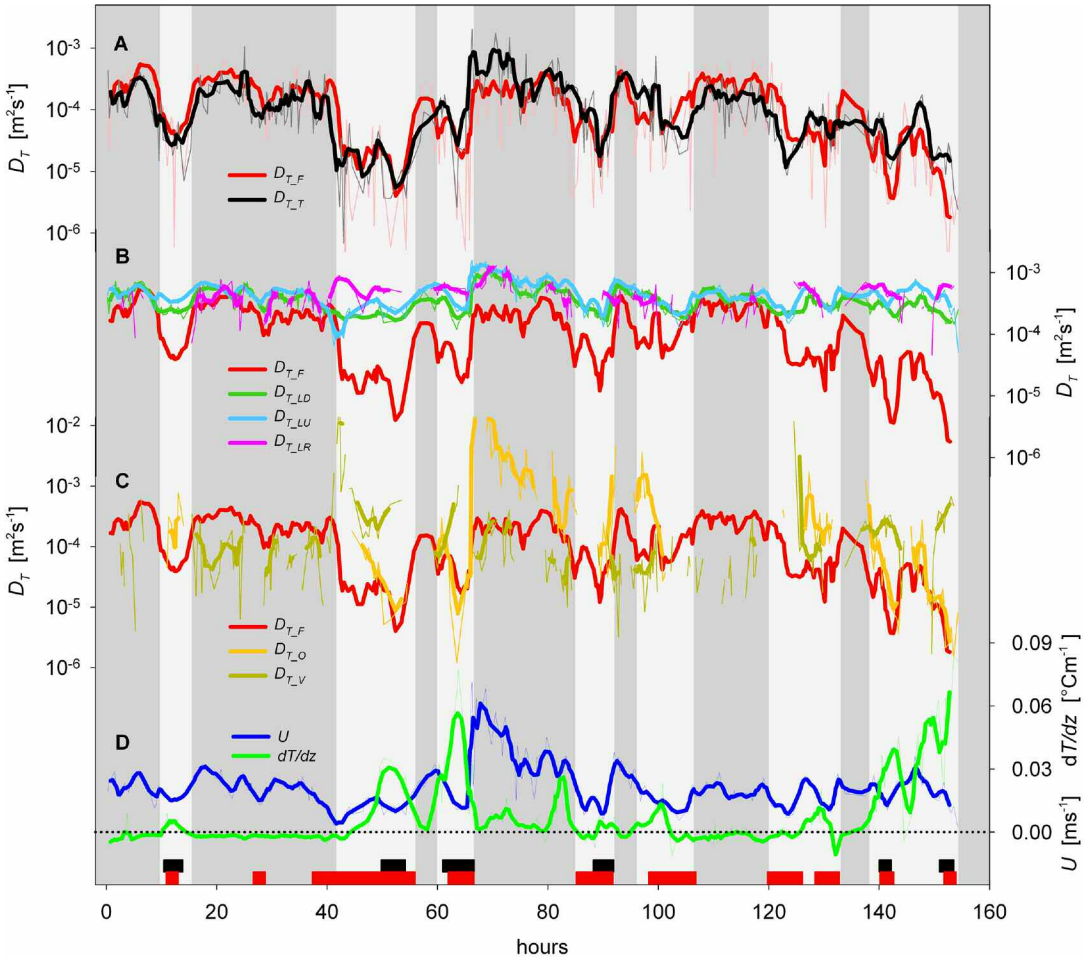

Fig. 4. Comparing turbulent diffusion coefficients derived from Fick's law (D_{T_F}) with estimates derived from (A): Taylor's hypothesis (D_{T_T}), from (B): the log-law and energy dissipation (D_{T_LD}), mean current velocities (D_{T_LU}), and Reynolds stress (D_{T_LR}), from (C): Osborn's equation (D_{T_O}) and turbulent viscosity (D_{T_V}). The lower panel (D) presents mean current velocity ($\bar{U}$) and the temperature gradient (dT/dz) between 0.5 and 1.5 m above the sediment. dT/dz above and below the dotted line (zero gradient) indicate stable and unstable stratification, respectively. Thin lines represent raw data and thick lines show a running average of four bursts. The light gray areas mark episodes where D_{T_LD}, D_{T_LU}, and D_{T_LR} strongly deviate from D_{T_F} and D_{T_T}. The red and black bars on the time axis denote periods with a Reynolds number below 10,000 and a gradient Richardson number (R_i) above 0.25, respectively (see discussion).

ε, $\bar{U}$, and $\partial\bar{U}/\partial z$ correspond with time periods of increased L_E, D_{T_T}, and D_{T_F}.

Fig. 6 shows three bursts (marked by the arrows in Fig. 5) that were analyzed in detail. Burst 97 and 167 were characterized by low but negative temperature gradients of -2×10^{-3} and -3×10^{-3}°C m^{-1}, respectively. The current velocity was increased during burst 97 (2.6 cm s^{-1}) and decreased during burst 167 (0.5 cm s^{-1}) (Fig. 6A). Burst 249 was characterized by moderate velocities (1.7 cm s^{-1}) and a strong positive temperature gradient of 4×10^{-2}°C m^{-1}.

Comparing burst 97 and 167, we observed a decrease of standard deviations of both, vertical velocity and temperature fluctuations from 1.9×10^{-3} to 1.3×10^{-3} m s^{-1} and from 2.5×10^{-5} to 1.8×10^{-5}°C (Fig. 6B + C), which corresponded to a decrease in current velocity. The temperature gradients during burst 97 and 167 were negative, which implies that the density gradients were positive and the resulting density fluxes negative. Comparing burst 97 and 167, the absolute density flux decreased by a factor of 7 from 2.1×10^{-10} to 3.0×10^{-11} W kg^{-1} and the resulting D_{T_F} decreased by a factor of ~10 from 4×10^{-4} to 4×10^{-5} m^2 s^{-1}. Although the density flux was very low during burst 167, it was consistent throughout the burst period as shown by the steady decrease of the integrated density flux (Fig. 6D small plot). The length scale L_E is presented in Fig. 6E in form of the integral of E_E plotted over the spatial distance r (see E8). With increasing r, the integral of E_E approached the first maximum (i.e., L_E). The decrease of L_E from 14 cm (burst 97) to 1 cm (burst 167) resulted in a significant decrease of D_{T_T}.

During burst 249, the strong positive temperature gradient stabilized the BBL causing strong temperature fluctuations (2×10^{-4}°C, Fig. 6C) and a pronounced positive density flux (6.5 ×

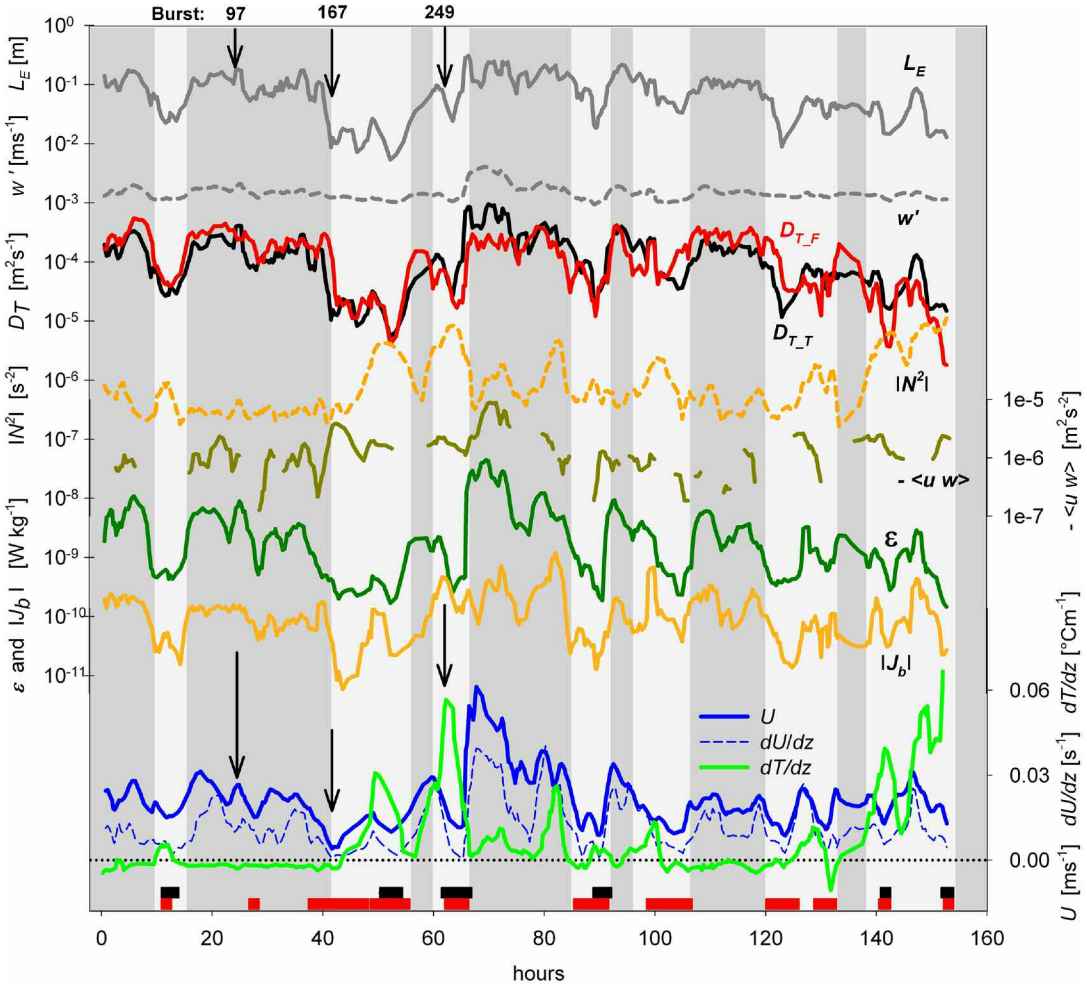

Fig. 5. Black and gray lines: time series of the Eulerian Lengthscale (L_E) and the standard deviation of the vertical velocity (w') contributing to D_{T_T}. In red and orange: time series of the buoyancy flux ($|J_b|$) and the Brunt-Väisälä frequency ($|N^2|$) contributing to D_{T_F}. For comparison, the dissipation rate (ε), Reynold stress (- <u w>), mean current velocity (U), velocity gradient (dU/dz), and temperature gradient (dT/dz) are shown. The light gray areas mark episodes where the log-law based estimates of D_t strongly deviate from D_{T_F} and D_{T_T}. The red and black bars on the time axis denote periods with a Reynolds number below 10,000 and a gradient Richardson number (R_i) above 0.25, respectively (*see* "Discussion"). Details of three individual bursts (arrows) are presented in Fig. 6.

10^{-10} W kg^{-1}, Fig. 6D). D_{T_F} during burst 249 was decreased by a factor of 5 compared with D_{T_F} during burst 97, when the BBL was not stably stratified. Furthermore, L_E decreased significantly to 5 cm at burst 249, which resulted in D_{T_T} that was comparable with D_{T_F} (6×10^{-5} and 8×10^{-5} m^2 s^{-1}, respectively).

Discussion

It is useful to divide the diffusivity models in our study (Table 1) into two categories. Models that describe diffusivity independently from boundary dimensions include the equations for D_{T_F}, D_{T_T}, D_{T_O}, and D_{T_V}. These so called free shear-flow models are basically applicable in all shear flows that produce stationary and homogeneous turbulence. Well established is the use of the Osborn model (D_{T_O}) in open ocean settings (Fennel 1995; Gregg et al. 1986) as well as in lakes (Lorke 2007), which involves the measurement of density gradients and kinetic energy dissipation. The second category of diffusivity models is only applicable for boundary flow, because these models depend on boundary dimensions. The model equations for D_{T_LU}, D_{T_LD}, and D_{T_LR} were all derived from the logarithmic law of the wall and can be summarized as log-law models. They offer different solutions for obtaining the shear velocity (u_*) according to Eq. 17, but they all scale with distance (z) to the sediment. The log-law is well established for high Reynolds number flows from numerous laboratory flume experiments and direct numerical simulations (Pope 2000).

Log-law models of turbulent diffusion

In our study, the different log-law models yielded similar diffusivities (Fig. 4) of which D_{T_LU} and D_{T_LD} agreed most while D_{T_LR} was less similar. This can be explained with the better correlation of current velocity ($\bar{U}$) and dissipation rate (ε)

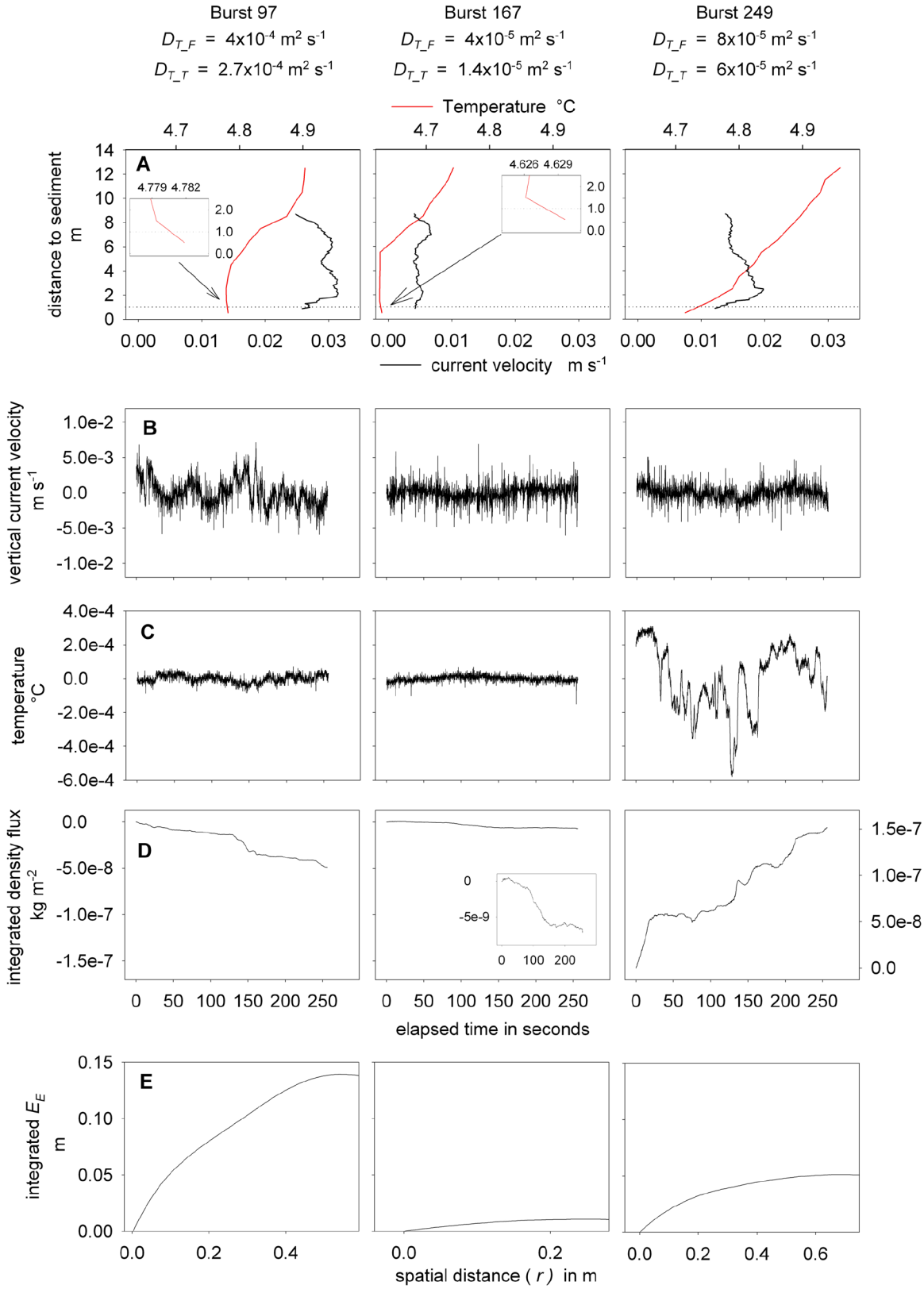

Fig. 6. From 3 bursts with distinct vertical gradients of temperature and current velocity (A), the velocity (B) and temperature (C) fluctuations as well as the integrated density flux, J_b, (D) and L_E (E) in the form of the integrated spatial correlation coefficient, E_E, are presented. The dotted line in (A) marks the height of the ADV sampling volume. The position of bursts in the time series are marked by arrows in Fig. 5.

when compared with the Reynolds stress $\langle uw \rangle$ (Fig. 5), because these quantities were used to determine D_{T_LU}, D_{T_LD}, and D_{T_LR}, respectively (Eq. 19 + Eq. 21 + Eq. 18). Estimates from log-law models agreed well with D_{T_F} at periods of no or unstable stratification. However, the log-law models could not account for a stable stratification. At transitions from unstable to stable stratification D_{T_LU}, D_{T_LD}, and D_{T_LR} stayed constant (Fig. 4), although a stable stratification should considerably decrease the diffusivity. In these cases, production and dissipation of turbulent kinetic energy are out of balance (see Eq. 20) and, thus, a condition for the log-law is no longer valid. In contrast, D_{T_F} was strongly affected by a stable stratification and decreased more than one order of magnitude. As a result, low D_{T_F} correlated well with high temperature gradients (Fig. 4). For this reason, and because Fick's law provides the most direct approach to determine diffusivity, we assumed that the estimates of D_{T_F} were correct and used D_{T_F} as reference for the other approaches.

Independent from a stable stratification, low current velocities strongly affected the diffusivity. D_{T_F} decreased rapidly when current velocities fell below ~1.5 cm s^{-1} (see D_{T_F} at hour 42, 85, and 125 in Fig. 4). For the critical velocity of 1.5 cm s^{-1}, a corresponding critical Reynolds number ($\mathrm{Re_c}$) of ~10,000 was calculated according to $\mathrm{Re} = z\bar{U} / \nu$, where z is the characteristic length scale that corresponds to the measurement height above the sediment (i.e., 1 m). For flows with $\mathrm{Re_c} < 10{,}000$ (red bars in Fig. 4 + 5), results from the log-law models strongly deviated from D_{T_F} and failed to give plausible diffusivities. As can be seen from Eq. 19, the log-law models predict diffusivities that decrease linearly with $\bar{U}$. However, the decrease of D_{T_F} at velocities below 1.5 cm s^{-1} was strongly nonlinear with respect to $\bar{U}$ (e.g., hour 42). In summary, the occasionally low flow velocities as well as the stable stratification caused the failure of the log-law models to predict plausible diffusivities.

Common free-shear-flow models of turbulent diffusion

Of the diffusivities from the free-shear-flow models, both, D_{T_O} and D_{T_V} deviated up to two orders of magnitude from D_{T_F} (Fig. 4). D_{T_V} was significantly higher than D_{T_F} at flow velocities with Reynolds numbers below $\mathrm{Re_c}$. At 42, 125, and 153 h, high D_{T_V} coincided with the change of current direction between upwelling and downwelling (Fig. 3). As a result, velocity gradients were close to zero and, therefore, below the resolution of the ADCP. At periods of unstable stratification D_{T_V} was well below D_{T_F}, whereas at periods of moderate stable stratification and increased current speed D_{T_V} agreed with D_{T_F}. In summary, D_{T_V} was not suitable to determine diffusivities under the present flow conditions, which in part, was due to the problematic measurements of velocity gradients. From the D_{T_O} model, reasonable estimates were calculated only for a stably stratified BBL. A useful criterion for the applicability of D_{T_O} was the dimensionless gradient Richardson number $Ri = N^2 / (\partial\bar{U} / dz)^2$, which describes the dynamic stability of a stratified shear flow. Based on perturbation analysis of parallel shear flow Miles (1961) deduced a critical value of Ri = 0.25, above which a stratified shear flow is sufficiently stable. We found that D_{T_O} was comparable to D_{T_F} whenever Ri was above 0.25 (black bars in Fig. 4). However, the requirement of a stable stratification for the D_{T_O} model certainly limits its applicability in boundary flows.

Taylor's model of turbulent diffusion

Of all applied models, diffusivities derived from Taylor's model (D_{T_T}) agreed best with diffusivities from Fick's law of diffusion (D_{T_F}). At flow regimes above as well as below $\mathrm{Re_c}$, D_{T_T} was comparable with D_{T_F} (Fig. 4). D_{T_T} was calculated as the product of the length scale L_E and the velocity w'. L_E may be interpreted as the characteristic eddy size that contains most of the turbulent kinetic energy. L_E varied from 1 to 30 cm and correlated with the mean current velocity (Fig. 5). At high mean current velocities, larger eddies were formed that contained more kinetic energy. As eddies fell apart, their energy cascaded down to smaller eddies until viscosity affected the flow and the energy dissipated into viscous shear. Large L_E therefore corresponded with increased dissipation rates (Fig. 5).

The characteristic size (L_E) of an eddy is associated with its characteristic velocity (w'). We defined the Reynolds number for energy containing eddies as $\mathrm{Re}_T = \mathrm{w}' L_E / \nu$, which is eventually the ratio of turbulent diffusivity to viscosity $\mathrm{Re}_T = D_T / \nu$. At stable stratification and decreased flow velocity (e.g., hour 50, Fig. 5), Re_T was around 10, a range where viscosity affects the flow. At such low flow, it is questionable if diffusivities on the basis of density flux measurements (D_{T_F}) were reliable. However, a consistent density flux throughout the burst period was observed for density fluxes as low as 10^{-11} W kg^{-1} (see also Burst 167 in Fig. 6D). Comparing D_{T_T} for high and low current velocities at negligible stratification (Burst 97 and burst 167 in Fig. 6), we observed a significant increase of L_E and a moderate increase of w' with increasing current velocities. However, when the BBL was stably stratified (Burst 249 in Fig. 6) L_E and w' were reduced.

The variability of diffusivities

In this study, the diffusivities derived from Taylor's model and from Fick's law varied over approximately three orders of magnitude from 1×10^{-3} to about 1×10^{-6} m^2 s^{-1} with logarithmic means of 6.7×10^{-5} and 8×10^{-5} m^2 s^{-1} for D_{T_F} and D_{T_T}, respectively (Fig. 7). In contrast, diffusivities derived from the log-law varied over not more than one order of magnitude with logarithmic means of 4.3×10^{-4} and 3.4×10^{-4} m^2 s^{-1} for D_{T_LD} and D_{T_LU}, respectively. This is because the log-law diffusivities depend linearly on the mean current velocity, which varied over approximately one order of magnitude (0.5-6 cm s^{-1}). D_{T_F} and D_{T_T} compared well with the highly variable diffusivities reported previously by Lorke (2007) for a shallow and stably stratified station in Lake Constance using Osborn's approach (D_{T_O}). However, most hydrodynamic studies in the BBL focus on estimating bottom stress (Dewey and Crawford 1988; Howarth and Souza 2005; Kim et al. 2000; Trowbridge et al. 1999) from which diffusivities may be derived using the log-law. Diffusivity measurements in the BBL that are not

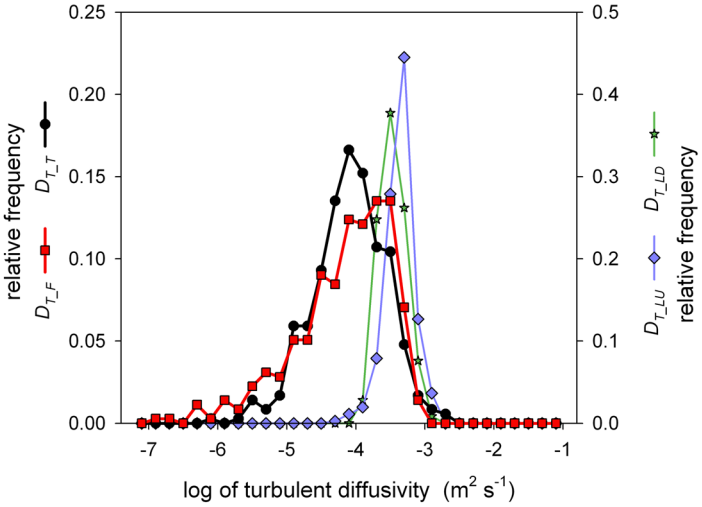

Fig. 7. Normalized frequency distribution of log10 turbulent diffusivities derived from different approaches.

based on the log-law (i.e., free-shear-flow models) are scarce, in lakes as well as in the ocean. Since the log-law does not apply for low current velocities and stratified shear flow, the low diffusivities that occur under these conditions are poorly described. However, the low turbulent diffusivities are of interest, because they can potentially result in bottom water hypoxia. As a rough estimate, we calculated that a turbulent diffusivity in the BBL of 1×10^{-6} m^2 s^{-1} above sediments with a moderate oxygen uptake of 20 mmol m^{-2} d^{-1} would result in an oxygen concentration gradient of ~ 230 µM m^{-1}. Because of the increased gradients, hypoxic conditions in the bottom water of lakes and the coastal ocean may occur in the first tens of centimeters above the sediment and subsequently increase the stress and mortality of the benthic fauna, even though sufficient oxygen can be found in the upper BBL. Because most shipboard-based measurements of oxygen concentrations cannot resolve the lower BBL, these kinds of hypoxic events may remain undetected. There is strong evidence that the extent and duration of hypoxic conditions in the coastal ocean are increasing (Diaz 2001; Diaz and Rosenberg 2008). A thorough description of the transport processes in the BBL would be beneficial to understand the evolution of hypoxic events in the bottom water.

Conclusions

From Taylor's theory (1921), we derived a new approach that allows determining the turbulent diffusivity in the BBL from high resolution velocity measurements. The diffusivities derived from the new approach (D_{T_T}) agreed well with those derived from gradient-flux measurements (D_{T_F}) whereas the common log-law models failed at decreased and stratified flow conditions. Our approach combines the broad applicability in free shear flows with a simple set up. A simple velocity measurement suffices to calculate D_{T_T} whereas the measurement of D_{T_F}, D_{T_V}, and D_{T_O} need at least additional gradient measurements.

When combined with solute gradient measurements (Holtappels et al. 2010), the new approach allows to determine the solute flux across the BBL according to Fick's law. This noninvasive flux measurement provides an alternative to the eddy correlation approach (Berg et al. 2003), which allows flux measurements only for a very limited number of solutes, measurable with high temporal and spatial resolution (e.g., oxygen via microsensors). However, solute gradients in the BBL decrease at high current velocities to eventually undetectable values, which limits the combined application of solute gradient and diffusivity measurements to low and moderate flows.

We showed that the new approach was capable to measure diffusivities at low current velocities as well as in stably stratified boundary layers. Under these conditions, diffusivities were much below the common estimates derived from the log-law. The decreased diffusivities question the common view that turbulent transport in the BBL is not affecting the flux across the sediment-water interface. Low turbulent diffusion in the BBL potentially controls the oxygen flux into the sediment. As result, turbulent diffusivities may not be seen as a mere quantity to calculate vertical fluxes. In fact, the focus is on the turbulent diffusivity itself and how it evolves during stratified and low flow conditions. Understanding the dynamics of turbulent transport in the BBL may be crucial to predict hypoxia in bottom waters and sulfide efflux from the sediments. The response of oxygen fluxes on variable current velocities and diffusivities, therefore, needs to be studied in more detail.

References

Appt, J., J. Imberger, and H. Kobus. 2004. Basin-scale motion in stratified upper Lake Constance. Limnol. Oceanogr. 49:919-933 [doi:10.4319/lo.2004.49.4.0919].

Berg, P., and others. 2003. Oxygen uptake by aquatic sediments measured with a novel non-invasive eddy-correlation technique. Mar. Ecol. Progr. Ser. 261:75-83 [doi:10.3354/meps261075].

Boudreau, B. P. 2001. Solute transport above the sediment-water interface, p. 104-126. *In* B. P. Boudreau and B. B. Jørgensen [eds.], The benthic boundary layer: Transport processes and biogeochemistry. Oxford Univ. Press.

Brand, A., D. F. McGinnis, B. Wehrli, and A. Wuest. 2008. Intermittent oxygen flux from the interior into the bottom boundary of lakes as observed by eddy correlation. Limnol. Oceanogr. 53:1997-2006 [doi:10.4319/lo.2008.53.5.1997].

Dade, B. D., A. Hogg, and B. P. Boudreau. 2001. Physics of flow above the sediment-water interface, p. 4-43. *In* B. P. Boudreau and B. B. Jørgensen [eds.], The benthic boundary layer: Transport processes and biogeochemistry. Oxford Univ. Press.

Dewey, R. K., and W. R. Crawford. 1988. Bottom stress estimates from vertical dissipation rate profiles on the continental-shelf. J. Phys. Oceanogr. 18:1167-1177 [doi:10.1175/

1520-0485(1988)018<1167:BSEFVD>2.0.CO;2].

Diaz, R. J. 2001. Overview of hypoxia around the world. J. Environ. Qual. 30:275-281 [doi:10.2134/jeq2001.302275x].

———, and R. Rosenberg. 2008. Spreading dead zones and consequences for marine ecosystems. Science 321:926-929 [doi:10.1126/science.1156401].

Fennel, W. 1995. A model of the yearly cycle of nutrients and plankton in the Baltic Sea. J. Mar. Syst. 6:313-329 [doi:10.1016/0924-7963(94)00031-6].

Gregg, M. C., E. A. Dasaro, T. J. Shay, and N. Larson. 1986. Observations of persistent mixing and near-inertial internal waves. J. Phys. Oceanogr. 16:856-885 [doi:10.1175/1520-0485(1986)016<0856:OOPMAN>2.0.CO;2].

Holtappels, M., M. Kuypers, M. Schlueter, and V. Bruechert. 2010. Measurement and interpretation of solute concentration gradients in the benthic boundary layer. Limnol. Oceanogr. Methods 9:1-13 [doi:10:4319/lom.2011.9.1].

Howarth, M., and A. Souza. 2005. Reynolds stress observations in continental shelf seas. Deep-Sea Res. II 52:1075-1086 [doi:10.1016/j.dsr2.2005.01.003].

Imboden, D. M., and A. Wüest. 1995. Mixing mechanisms in lakes, p. 83-138. *In* A. Lerman, D. M. Imboden, and J. Gat [eds.], Physics and chemistry of lakes. Springer-Verlag.

Ivey, G. N., K. B. Winters, and J. R. Koseff. 2008. Density stratification, turbulence, but how much mixing? Annu. Rev. Fluid Mech. 40:169-184 [doi:10.1146/annurev.fluid.39.050905.110314].

Kim, S. C., C. T. Friedrichs, J. P. Y. Maa, and L. D. Wright. 2000. Estimating bottom stress in tidal boundary layer from Acoustic Doppler Velocimeter data. J. Hydraul. Eng. ASCE 126:399-406 [doi:10.1061/(ASCE)0733-9429(2000)126:6(399)].

Lorke, A. 2007. Boundary mixing in the thermocline of a large lake. J. Geophys. Res. Oceans 112, C09019, 10 PP [doi:10.1029/2006JC004008].

———, and A. Wüest. 2005. Application of coherent ADCP for turbulence measurements in the bottom boundary layer. Journal of Atmospheric and Oceanic Technology 22: 1821-1828.

———, L. Umlauf, T. Jonas, and A. Wuest. 2002. Dynamics of turbulence in low-speed oscillating bottom-boundary layers of stratified basins. Environ. Fluid Mech. 2:291-313 [doi:10.1023/A:1020450729821].

———, L. Umlauf, and V. Mohrholz. 2008. Stratification and mixing on sloping boundaries. Geophys. Res. Lett. 35, L14610, 5 PP [doi:10.1029/2008GL034607].

Miles, J. W. 1961. On the stability of heterogeneous shear flows. J. Fluid Mech. Dig. Arch. 10:496-508.

Osborn, T. R. 1980. Estimates of the local rate of vertical diffusion from dissipation measurements. J. Phys. Oceanog. 10:83-89.

Pope, S. B. 2000. Turbulent flows. Cambridge Univ. Press.

Sato, Y., and K. Yamamoto. 1987. Lagrangian measurement of fluid-particle motion in an isotropic turbulent field. J. Fluid Mech. 175:183-199 [doi:10.1017/S0022112087000351].

Sauter, E. J., M. Schlueter, J. Wegner, and E. Labahn. 2005. A routine device for high resolution bottom water sampling. J. Sea Res. 54:204-210 [doi:10.1016/j.seares.2005.04.005].

Taylor, G. I. 1921. Diffusion by continuous movements. Proc. London Math. Soc., 2, 196-211 <http://www.aos.princeton.edu/WWWPUBLIC/gkv/history/Taylor21.pdf>.

———. 1938. The spectrum of turbulence, p. 476-490. *In* Proceedings of the Royal Society A 164:476-490.

Tennekes, H., and J. L. Lumley. 1972. A first course in turbulence. MIT Press.

Trowbridge, J. H., W. R. Geyer, M. M. Bowen, and A. J. Williams. 1999. Near-bottom turbulence measurements in a partially mixed estuary: Turbulent energy balance, velocity structure, and along-channel momentum balance. J. Phys. Oceanogr. 29:3056-3072 [doi:10.1175/1520-0485(1999)029<3056:NBTMIA>2.0.CO;2].

von Kármán, T. 1930. Mechanische Ähnlichkeit und Turbulenz, p. 85-105. *In* Proceedings of the Third International Congress of Applied Mechanics, Vol 1, Norstedt and Sons, Stockholm.

Wollast, R. 1991. The coastal organic carbon cycle: fluxes, sources and sinks, p. 365-381. *In* J.M.M.R.F.C. Mantoura and R. Wollast [eds.], Ocean margin processes in global change. John Wiley & Sons.

Wuest, A., and A. Lorke. 2003. Small-scale hydrodynamics in lakes. Annu. Rev. Fluid Mech. 35:373-412 [doi:10.1146/annurev.fluid.35.101101.161220].

Submitted 20 May 2010
Revised 3 November 2010
Accepted 6 December 2010